Measurement of Quantum Jumps of a Ba 138+ electron

Michael Clancy, University of Washington INT REU
Advisor: Boris Blinov

Abstract

The collapse of the wave function is studied by measuring the state of an electron in a Barium 138^+ ion. The state of the electron is driven between energy eigenstates by lasers, and the fluorescence at the wavelength of a single transition is used for measurement of the state. An algorithm is developed to detect jumps in the time series data. Non-instantaneous collapse is observed, but can be explained by the limitations of the algorithm.

1 Introduction

Quantum mechanics is the most thoroughly tested and verified theory in all of modern science, and yet its foundational principles are still poorly understood. Perhaps the greatest of these gaps in present understanding is the measurement problem, which can be described in the following example: Suppose we want to know the state of a particle of mass m in a 1-D infinite square well of width a. One can solve for the eigenfunctions of the free particle Hamiltonian subject to the condition $\psi(x) = 0$ outside of $x = 0$ and $x = a$:

$$\psi_n(x) = \sqrt{\frac{2}{a}} \sin \frac{n\pi x}{a}, \qquad n = 1, 2, ... \tag{1}$$

with energy eigenvalues $E_n = \frac{n^2\pi^2\hbar^2}{2ma^2}$ [1]. The Hilbert space $\mathcal{H}$ associated with this system is the set of all square-integrable functions $\psi : [0, a] \longrightarrow \mathbb{C}$, and the states of the system can be represented by functions $\psi \in \mathcal{H}$ such that ψ' is continuous and $\int_0^a |\psi(x)|^2 = 1$.[1] If one takes any such state of the system ψ, it can be written in terms of the energy eigenfunctions (also called eigenstates):

$$\psi = \sum_{n=1}^{\infty} \langle \psi_n, \psi \rangle \psi_n \tag{2}$$

Separately, one can solve for the time evolution operator $U(t)$ according to Schrödinger's equation:

$$i\hbar \frac{dU}{dt} = \hat{H}U \tag{3}$$

The state $\Psi(t)$ is then given by the equation $\Psi(t) = U(t)\Psi(0)$, taking the state at time 0 to be $\Psi(0) = \psi$. With this time evolution operator, we can

[1] A more careful treatment involving density operators and the energy spectrum is required for the analysis of measurements in more general cases, but is not required for preliminary discussion. In particular, entangled states present difficulties in treating the state of a system as a wavefunction. [2, 3].

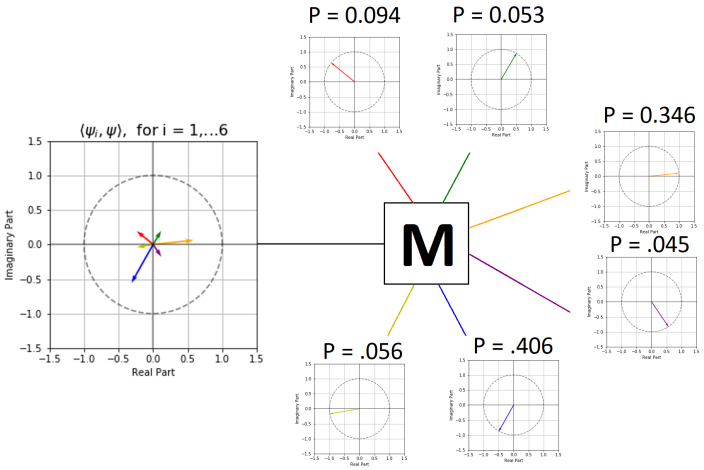

Figure 1: Representation of projective measurement. An initial state ψ in a 6-dimensional Hilbert space has 6 complex coefficients in an arbitrary basis. These coefficients are represented by different colored arrows in the complex plane. After being measured by the box M, the state collapses into one of the eigenstates with probabilities given by the squared length of the arrows.

see there is nothing random about quantum mechanics as far as Schrödinger's equation goes. Even the uncertainty principle is not a statement about the randomness of quantum mechanics: randomness only occurs upon measurement of a quantum state. When a scientist conducts an experiment to measure the energy of the of the state ψ at some time t, he or she does not measure a superposition of energy eigenvalues: they measure only one eigenvalue, and the probability with which they measure the eigenvalue E_n is given by $|\langle\psi_n, \psi\rangle|^2$. Similarly, the state of the system right after measurement is ψ_n. In this way, the act of measuring the energy of a system in a superposition of energy eigenstates acts to "project" the initial state into just one of the eigenstates, with probabilities given by the squared modulus of the coefficients of the state as expressed in the energy eigenbasis. This simple projective measurement postulate was developed by von Neumann [4], and a novel illustration is provided in Figure 1. This wave function collapse — the process by which ψ becomes ψ_n for some n — still has no experimentally determined physical mechanism or interpretation. The Copenhagen interpretation is sufficient from a practical point of view: there is no proposed mechanism, collapse simply *happens*, and the process of collapse is tacked onto Schrödinger's equation to describe the results of experiments. The many-worlds interpretation [5] is, stated quite loosely, that all of these measurement results occur, but in different universes with different observers: the universe "branches out" every time such a measurement is performed. Deco-

herence has been an enourmously successful theory (which postulates nothing extra about quantum mechanics) in describing the appearance of wave function collapse in certain situations [6–8], but it has been shown that it does not solve the measurement problem entirely [9, 10]. One of the greatest roadblocks in understanding this problem of connecting theory with measurement is the lack of a precise physical definition for the word "measurement"; despite being the fundamental connection between theory and experiment. In this paper, the state of the electron in a Ba 138^+ ion in an ion trap is measured by detecting its fluorescence at 493 nm (see Fig 2) with a photomultiplier tube (PMT). More specifically, the ion is subjected to 1762 nm light, driving a Rabi Oscillation (between the "ground" $|g\rangle := 6S_{1/2}{}^2$ and "excited" $|e\rangle := 5D_{5/2}$ states). During a Rabi oscillation, the ion can be in a superposition of the ground and excited states, like the state $\psi = \frac{1}{\sqrt{2}}(|g\rangle + |e\rangle)$. The state ψ can be measured by shining 493 nm light on the ion, "collapsing" the state ψ into either $|g\rangle$ or $|e\rangle$ with equal probability. If the electron collapses into $|g\rangle$, then it absorbs a 493 nm photon and is excited into the $6P_{1/2}$ state (not the excited state $|e\rangle$). The $6P_{1/2}$ state rapidly decays back into the $|g\rangle$ or into the $5D_{3/2}$ state, with a 3:1 branching ratio, respectively [11]. In order to keep the electron out of the $5D_{3/2}$ state, 650 nm light is also applied to excite the electron back into the $6P_{1/2}$ state. The ion will repeatedly cycle through this manifold, continually emitting 493 nm light to be detected at the PMT. If the ion collapses into the state $|e\rangle$, then it will be unaffected by the 493 and 650 nm light, and any counts on the PMT are simply noise. In order to measure any arbitrary superposition state, then, 493 nm light is sent to the ion, the signal is recorded for some time after, with high counts showing that the ion collapsed into the ground state, and low counts showing that the ion collapsed into the excited state. For this reason, the ground and excited states will be referred to as the "bright" and "dark" states, respectively.

If all three of the wavelengths in Figure 2 are incident on the ion at once, then the ion will rapidly get shelved into and deshelved from the state $|e\rangle = 5D_{5/2}$. These jumps are historically called "Quantum Jumps" or "telegraphing" [12]. In this paper, we present the results of measuring the fluorescence of the ion while executing these jumps with 50 ms time bins in a linear Paul trap, and discuss plans to measure the photon counts on a smaller time scale, in a parabolic mirror trap with better light collection efficiency. This fluorescence fits the bill for a projective measurement ($\frac{1}{\sqrt{2}}(|g\rangle + |e\rangle) \longrightarrow |g\rangle$ or $|e\rangle$), and this measurement technique has been used in the Blinov lab [11] to demonstrate a violation[3] of Bell's inequality, further validating its treatment as a measurement in the mathematical formalism. In this paper, we study if there is any physical process that happens when this projective measurement occurs.

[2] We have adopted the notation nL_j to denote the state with quantum numbers n,l, and j [1]: n being the principal quantum number, l the azimuthal quantum number, and j the angular momentum quantum number. A magnetic field is applied to the trap, so these "eigenstates" are actually sub-manifolds, but this detail is not important for preliminary discussion.

[3] The Bell's inequality violation appearing in [11] closed the detection loophole, but not the locality loophole.

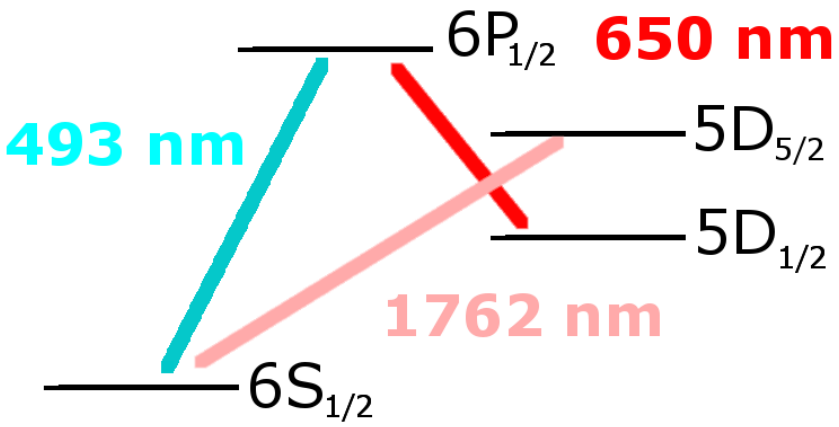

Figure 2: Energy diagram of Ba 138^{+}.

2 Setup

2.1 Ion Traps

An ion trap is an apparatus capable of trapping single atoms with excess charge. Two Paul traps were utilized to measure the quantum jumps: a linear Paul trap, and a parabolic mirror ion trap. The linear trap was used to collect data for a preliminary analysis of results, which will be used in the future for experiments with the parabolic mirror trap. The parabolic mirror has approximately 40% solid angle light collection efficiency, which allows for high time resolution in data collection. The details of the procedure for trapping are described in [11], but a general outline is provided here.

The parabolic mirror trap is a deformed version of the traditional ring trap used in ion trapping experiments, as shown in Figure 3. The trap is under Ultra High Vacuum (UHV) with a pressure of less than 10^{-11} Torr. A ceramic tube containing barium is wrapped in tungsten wire, and current is run through that loop. This high temperature evaporates barium atoms, which then move

Figure 3: Parabolic mirror trap. On the left is a traditional ring trap, with two needle electrodes to which a DC voltage is applied, and a ring to which a Radio Frequency (RF) oscillating voltage is applied (approximately 11.7 MHz for this trap). This creates a time-averaged pseudo-harmonic potential, so that the ion stays in place. On the right is the parabolic mirror, whose resulting potential does not have a nice closed form, but produces a similar effective trapping potential in the center of the trap [11]. Figure courtesy of [11].

toward the center of the trap. At this point, two ionization lasers, at 791 nm and a 337 nm, are used to ionize the most common isotope of Barium, Ba 138, into Ba 138^+ [11]. The Ba 138 isotope has no nuclear spin, simplifying the energy diagram. After being ionized, the Ba 138^+ is hydrogen-like, with a charge of $+e$. The ionization is done at the bottom of the potential well induced by a Radio Frequency (RF) field, trapping the ion in the center. In order to keep the ion from gaining too much vibrational energy from the potential and other sources of heating, the ions are cooled by means of a technique called Doppler cooling. Doppler cooling works in the following way: Assume the ion has some momentum p in the $\hat{\mathbf{x}}$ direction, $\vec{p} = p\,\hat{\mathbf{x}}$. Assume also that there is some wavenumber k associated with one of the internal atomic transitions of the outer electron in the ion. Then one can shine laser light on the ion, with momentum $\hbar(k-\epsilon)\hat{\mathbf{x}}$ in the lab frame, from the positive x direction. Since the ion is moving toward the light, it will see the light slightly blue-shifted back toward the resonant frequency of the transition, and absorb the momentum of the incident photon, resulting in a new momentum $(p-\hbar(k-\epsilon))\hat{\mathbf{x}}$. If the excited state of the transition is not stable, then another photon will be emitted in a random direction. This will happen millions of times per second (depending on the intensity of the incident laser light), resulting in an ion with very low temperature in the center of the trap. The 493 nm light, in addition to being the primary source of cooling, is used as a method for state detection, as described in the introduction. An interference filter is used to filter out light of other wavelengths. When the ion is in the focus of the parabolic mirror, which covers a solid angle of approximately 40% of 4π steradians, approximately 40% of the re-emitted 493 nm light is then refocused by a 40 cm converging lens onto

the Photo-Multiplier Tube (PMT), which is able to detect single photons with approximately 20% quantum efficiency.

3 Procedure

In order to prevent damage to the surface of the parabolic mirror from the bombardment of barium atoms, initial loading of the trap is done 1.98 mm in front of the focus of the mirror on the axis of the needle (see Figure 3). The needle is then pulled back axially, and DC voltages are applied to bias plates just above the mirror for radial control of the ion position. After the ion is placed in focus, it is subjected to the 493, 650, and 1762 nm lasers simultaneously. The interaction of the ion with the 1762 nm light is treated semi-classically. The Hamiltonian of this interaction, $\hat{H}_I$, is treated as a time dependent perturbation to the Hamiltonian $\hat{H}_0$ of the atom for a system whose two states are the corresponding ground and excited state of the transition induced by the 1762 nm light. The total Hamiltonian and interaction Hamiltonian are, respectively:

$$\hat{H}(t) = \hat{H}_0 + \hat{H}_I(t) \tag{4}$$

$$\hat{H}_I(t) = e\mathbf{E} \cdot \mathbf{r} \tag{5}$$

for a dipole moment of $e\mathbf{r}$ for the atom. If the particle starts in the ground state $|g\rangle$, and the 1762 nm laser is tuned to exactly the resonant frequency of the transition $6S_{1/2} \rightarrow 5D_{5/2}$, one can solve Schrödinger's equation for the time dependent Hamiltonian $\hat{H}(t)$ in Equation 4 to obtain the state as a function of time [11]:

$$\psi(t) = c_g(t)|g\rangle + c_e(t)|e\rangle \tag{6}$$

with:

$$|c_g(t)|^2 = \cos^2 \frac{\Omega t}{2} \tag{7}$$

and:

$$|c_e(t)|^2 = \sin^2 \frac{\Omega t}{2} \tag{8}$$

where the parameter Ω is called the Rabi Frequency, and is proportional to the magnitude of the electric field and the dipole moment of the ion [11]. It is the frequency of the oscillation between the ground and excited states of the transition. If the state of the ion is measured while in the "middle" of such an oscillation, the electron has 50% probability of collapsing into either of the $|g\rangle$ or $|e\rangle$ energy eigenstates.

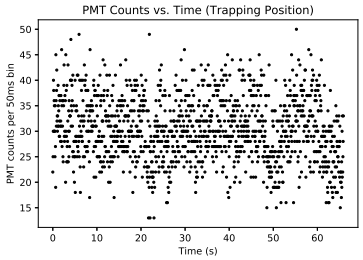

(a) Time Series of PMT counts for 50 ms bins.

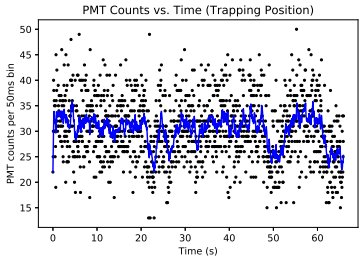

(b) Time series of PMT counts for 50 ms bins with a smoothing filter applied.

Figure 4: Telegraphing of an ion in a parabolic mirror trap.

4 Results

4.1 Parabolic Mirror Trap

The ion was not successfully pulled back into the focus using the procedures described in Section 3. However, proof-of-concept data was taken for the ion in its original trapping position. After trapping, the ion is exposed to the 1762 nm laser light as well as the cooling lasers, and data is recorded using LabView software with hardware timing and 50 ms bins.

If the 1762 nm laser is at the right intensity and properly aligned, the ion will transition[4] between bright and dark more rapidly than the time resolution can show, resulting in a moderately bright signal. Therefore, the 1762 nm laser is slightly misaligned so that less frequent telegraphing can be observed.

The telegraphing can be seen in Figure 4. In order to further motivate the completion of this experiment in the parabolic mirror trap, a linear Paul trap being used for other experiments in the Blinov lab was implemented.

4.2 Linear Trap

In the linear trap, data was recorded using LabView with software timing[5] and 50 ms bins. The ion rapidly switches between the dark and bright state, as can be seen in Figure 5a. The ion clearly spends more time in the bright state, which can be intuitively understood - while the ion is fluorescing, it spends a lot of time in the $6P_{1/2}$ and $5D_{3/2}$ states —away from the ground state, so that it is isolated from interaction with light at 1762 nm, and therefore isolated from transitioning into the $5D_{5/2}$ state. While in $5D_{5/2}$ state, however, the 1762 nm

[4]This is an abuse of the word "transition". This does not refer to actual atomic transitions, but to macroscopic changes in brightness.

[5]The tickrate of the LabView software is about 1 kHz. This becomes an issue for time bins on the order of 10 ms.

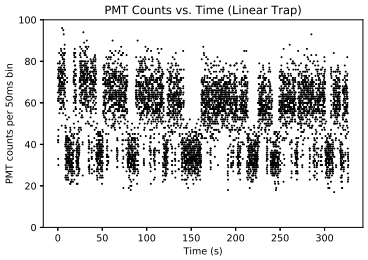

(a) Time series for linear trap. Data was collected for 6537 bins of length 50 ms, for a total of 326.95 seconds runtime.

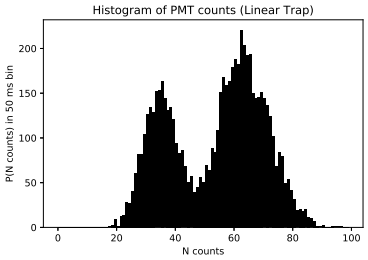

(b) Histogram of photon counts per 50 ms bin. Overlap between bright and dark curves at N = 46. 2240 data points had less than 46 counts, resulting in a measurement of the ion spending approximately 34.6% in the $5D_{5/2}$ state.

Figure 5: Time series and histogram of ion fluorescence in linear trap.

light is always driving the transition back into the ground state. This results in many small "dips" which can be seen in Figure 5a.

4.3 Jump Analysis

A simple jump detection algorithm was developed in order to analyze the behavior of the electron during these transitions. The jump detection algorithm was implemented as follows.

The time series data is denoted by (x_i, t_i), $i = 1, 2, ..., n$ (with $n = 6537$). For each index i in the time series, a new calculated sequence y was determined by the equation:

$$y_i = \Big(\frac{1}{l}\Big(\sum_{j=i-l}^{i-1} x_j - \sum_{k=i}^{i+l-1} x_k\Big)\Big)^2 \tag{9}$$

Each value y_i essentially compares the previous data points to the next data points by comparing the difference in the mean before and after an index. The parameter l is the radius of the neighborhood that the algorithm checks, and was chosen by inspection to be $l = 7$. If any of these y_i's are greater than a cutoff c_0 (chosen by inspection to be 150), then an index is initially detected as a jump. That is, the set of preliminary jump indices J_0 is given by:

$$J_0 := \{i : y_i > c_0\} \tag{10}$$

This initial set of jump indices J_0 is refined in two steps. Firstly, in addition to picking out jump indices, Equation (9) picks out some of its neighbors. This can be fixed by changing the cutoff, but the signal is noisy. Therefore, a radius

$r = 3$ indices is chosen so that only the index which locally maximizes the difference appearing in Equation 9 is kept. That is, a new set of indices is determined by the equation:

$$J_1 := \{j \in J_0 : y_j = max(y_{j-r}, ..., y_j, ..., y_{j+r})\} \tag{11}$$

The second refinement of jump detection indices is done by removing indices due to noise, or indices of jumps which occur too quickly to analyze. The latter are of enormous interest, but are beyond the scope of this experiment, and require greater time resolution which may be achieved with the parabolic mirror trap. In order to pick out these indices, we check whether or not the signal changed by more than a cutoff c_1 before and after the jump. To say this precisely, we first develop the following notation: Let $j \in J_1$. Then j^+ is defined as the next largest element of J_1, and j^- is the next smallest element. We also make the natural definitions that 0^+ is the smallest element of J_1, and if j is the largest element of J_1, then j^+ is defined as the largest index of the time series. Then we define a partition of the data set x_i by the equation [6]:

$$P(J_1) := \{p_j := \{x_i : j \leq i < j^+\}, \text{ for each j} \in J_1 \cup \{0\}\} \tag{12}$$

The following definition will also be useful:

$$\mu(p_j) := \frac{1}{j^+ - j} \sum_{i \in p_j} x_i \tag{13}$$

The set of jump indices is finally defined to be:

$$J := \{j \in J_1 : \left|\mu(p_j) - \mu(p_{j^-})\right| \geq c_1\} \tag{14}$$

The effectiveness and limitations of this jump detection algorithm are illustrated in Figure 6.

In Figure 6b, it can be clearly seen that the ion transitions back and forth more rapidly than the 50 ms time bins can resolve. This is perhaps not entirely surprising: the Rabi frequency of this transition is on the order of microseconds for this intensity [13], and the separation between scattering events of 493 nm photons is on the order of nanoseconds [13]. From this result alone we can conclude that our time resolution is too coarse for a complete characterization of processes involved in state transitions. Nevertheless, these quick transitions back and forth can be treated as noise, and the jumps which can be resolved by this scheme can still be analyzed.

The first description of the data that can be made using the jump detection algorithm is the histogram of time between jumps (the distance between each red line). The set TBJ (time between jumps) is defined by the equation:

$$TBJ = \left\{t_{j^+} - t_j : j \in J - \{max(J)\}\right\} \tag{15}$$

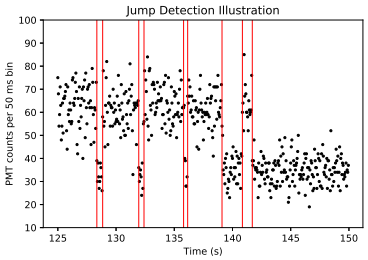

(a) An illustration of the effectiveness of the jump detection algorithm.

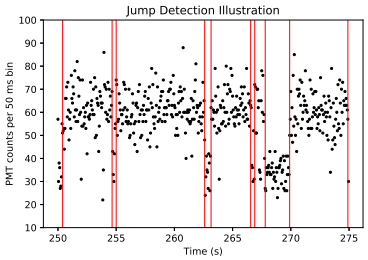

(b) An illustration of the limitations of the jump detection algorithm. Between 250 and 255 seconds, there is very clear rapid switching between bright and dark.

Figure 6: Sections of the entire time series are plotted, and vertical red lines indicate a detected jump index.

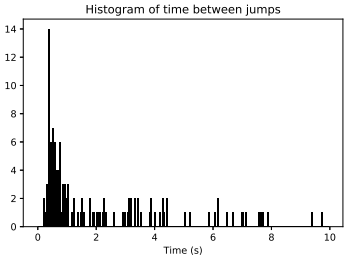

(a) Histogram of times between jumps.

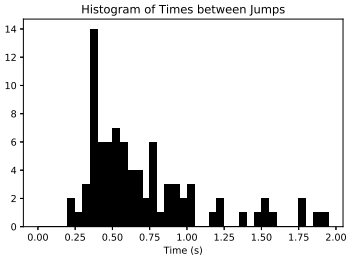

(b) Histogram of times between jumps between 0s and 2s.

Figure 7: Histogram of time between jumps, observed on a large and small time scale.

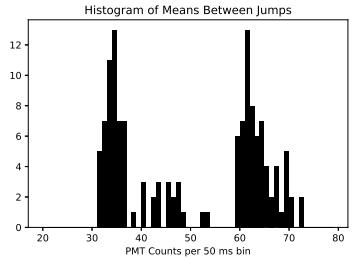

(a) Means Between Jumps

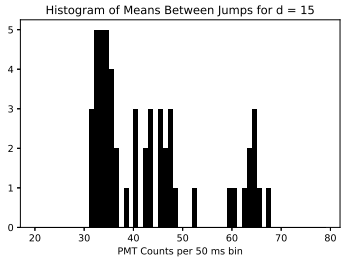

(b) Means Between Jumps for short partition elements, d = 15

Figure 8: Means Between Jumps

The histogram of TBJ is shown in Figure 7.

It is evident from Figure 7 that the vast majority of the times between jumps are just a few hundred milliseconds or less. There is a sharp spike at $350\text{ms} = 7 * (50\text{ms})$ — this is an artifact of the choice $l = 7$. Further, we can verify the observation that short elements of the partition happen when the ion is dark. First, we define a new partition $P(J)$ according to (12). Next, we make the reasonable definition as for "short" as less than 750ms. Therefore, we define the parameter $d = 15$, so that elements of the partition $P(J)$ which are less than d long can be picked out of the entire partition. Then we can define this subset of the partition by:

$$P_d(J) = \{p_j \in J : j^+ - j < d\}. \tag{16}$$

Then we may calculate the mean of the signal during these short elements of the partition, the Means Between Jumps for a cutoff d (MBJ_d) by the definition:

$$MBJ_d = \left\{\mu(p_j) : p_j \in P_d(J)\right\} \tag{17}$$

From (17) follows the natural definition that $MBJ := MBJ_\infty$. The histograms for MBJ and MBJ_{15} are shown in Figure 8.

In Figure 8b it is shown that the majority of short partition elements have a dark mean, illustrating that the "dips" into the dark state occur more often than "spikes" into the bright state.

There are three clear peaks in Figure 8a. These peaks can be distinguished by placing dividers at $\chi_D = 38$ counts and $\chi_B = 56$ counts, with the bins created by these dividers representing dark, intermediate, and bright partition elements. Intermediate partition elements correspond to quick telegraphing which cannot be resolved by the 50 ms time bins.

[6]The less than or equals on being on the left is because the jump should represent when the signal changed "states".

We are interested in how the electron behaves at times near the detected jumps. Suppose we are looking at jumps from the bright state into the dark state, and suppose the particular index of that jump is j. Then we would like to check if x_{j+1} is any different from the ordinary dark signal - that is, are the PMT counts still slightly higher after the jump has already occured? We could ask similar questions about x_{j+2}, x_{j-1}, and so on, as well as looking at dark to bright jumps. Unfortunately, there is too much variation in any single trial to address such a question. Information must be extracted from the mean of many such trials. In order to make this discussion precise, let us make the following definitions. First, we want to determine what defines a bright state and what defines a dark state. To do this, we define the dark indices and bright indices by the equations:

$$I_D := \{i : \mu(p_j) < \chi_D\} \tag{18}$$

and

$$I_B := \{i : \mu(p_j) > \chi_B\} \tag{19}$$

and for each i, j is such that $j \leq i < j^+$. These may be used to calculate the mean bright and dark signal:

$$\mu(D) := \frac{1}{N(I_D)} \sum_{i \in I_D} x_i \tag{20}$$

$$\mu(B) := \frac{1}{N(I_B)} \sum_{i \in I_B} x_i \tag{21}$$

with $N(A)$ for a set A denoting the number of elements in that set. These were calculated to be $\mu(D) = 34.486$ and $\mu(B) = 63.407$. With these tools we may define which jump indices correspond to jumps in a particular direction[7]:

$$J_{DB} := \{j \in J : \mu(p_{j^-}) < \chi_D \qquad \text{and} \qquad \mu(p_j) > \chi_B\} \tag{22}$$

and

$$J_{BD} := \{j \in J : \mu(p_{j^-}) > \chi_B \qquad \text{and} \qquad \mu(p_j) < \chi_D\} \tag{23}$$

J_{DB} is the set of jump indices such that the mean of the partition element before the jump was dark and the mean of the partition element after was bright, where "was dark" means it was less than the cutoff χ_D, as determined by inspection of the histogram in Figure 8a, and similarly for "was bright". J_{BD} is the set of jumps where the ion was bright before and dark after.

We then make the definitions:

$$I^{DB}_{j+\Delta} := \{i : i = j + \Delta \qquad \text{for some} \qquad j \in J_{DB}\} \tag{24}$$

[7]With "direction" meaning bright $\rightarrow$ dark, or dark $\rightarrow$ bright.

and

$$I^{BD}_{j+\Delta} := \{i : i = j + \Delta \qquad \text{for some} \qquad j \in J_{BD}\} \tag{25}$$

The set $I^{DB}_{j+\Delta}$ is the set of indices which are Δ more than each jump index $j \in J_{DB}$ from dark to bright. $I^{BD}_{j+\Delta}$ is the same set for bright to dark jumps. The parameter Δ may be negative or positive, depending on whether one wants to look at data before or after a jump. For example, the set I^{BD}_{j+1} is the set of indices appearing immediately after the index of each jump from the bright state to a dark state in the entire data set.

Of particular interest are the numbers $\mu(I^{\alpha\beta}_{j+\Delta})$ for values of Δ ranging from -4 to 4, and $\alpha, \beta = D, B$. Larger values of Δ start picking up information from the other state for short partition elements, as the smallest element of TBJ is 200 ms. If we want to compare the means of these sets to the regular bright and dark signals, we make the definition:

$$\mu^*(I^{\alpha\beta}_{j+\Delta}) = \begin{cases} \mu(\alpha) & \text{if} \quad \Delta < 0 \\ \mu(\beta) & \text{if} \quad \Delta \geq 0 \end{cases} \tag{26}$$

Equation 26 is of utmost importance in analyzing the change in signal before and after each jump. It is simple to state in words with an example: If I am concerned with dark to bright jumps (DB), and pick $\Delta = -1$, then I will want compare the mean of the indices right before each jump index to the mean of the dark state. If I want to look at DB jumps with a positive value for Δ, I will want to compare that mean to the mean of the bright state, and Equation 26 is a way of simultaneously stating this for each case.

Plotted in Figure 9 is $\mu(I^{\alpha\beta}_{j+\Delta}) - \mu^*(I^{\alpha\beta}_{j+\Delta})$, for $\Delta = -4, ..., 4$ and $\alpha, \beta = D, B$. This represents the difference in the signal from the expected value of the signal around a jump index.

Under the assumption that the jump detection algorithm is perfectly robust, Figure 9 suggests that if the ion is in the dark state, then just before jumping into the bright state, the signal (on average) ramps up over the course of approximately 200 ms. Similarly, if the ion starts in the bright state, then after jumping into the dark state, it takes a few indices to ramp down. This result is likely a byproduct of the imperfection of the jump detection algorithm. For example, defining $x(I) := \{x_i : i \in I\}$, we may look at the sets $x(I^{BD}_{j+0})$ and $x(I^{BD}_{j+4})$. The histograms of these sets are plotted in Figure 10.

The means of these data sets appear in Figure 9. A bimodal distribution appears in Figure 10a, which suggests that the jump detection algorithm happened too early or too late, and Figure 9 is simply a display of the limitations of the algorithm. Finer time resolution is needed to answer the questions posed by these results.

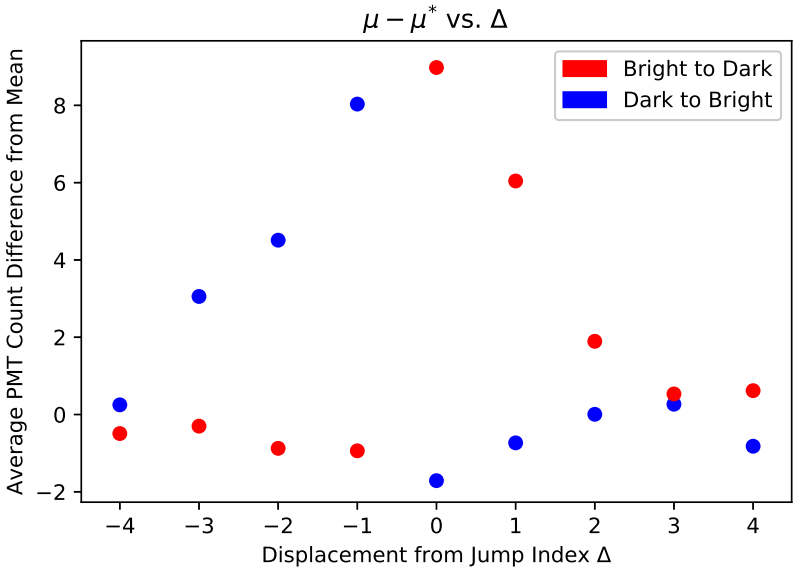

Figure 9: Plot of the mean signal difference from the expected value around each jump index.

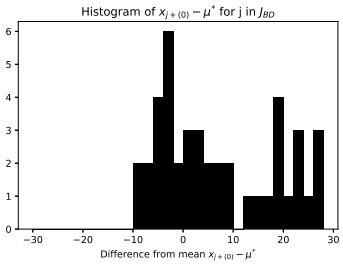

(a) Histogram of data points at jump indices for bright to dark transitions.

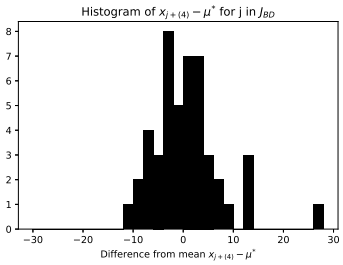

(b) Histogram of data points at j+4 indices, for bright to dark transitions.

Figure 10: Histogram of data points around jump indices.

5 Conclusion and Future Work

In a linear Paul trap with 50 ms time bins, the PMT counts displaying the fluorescence of a Ba 138^+ ion do not appear to represent an instantaneous quantum jump, as analyzed by a jump detection algorithm. This result is inconclusive, and further experiments will be able to either replicate the non-instantaneous collapse, or obtain different results, suggesting the results appearing in this paper are an artifact of the limitations of the implemented jump detection algorithm. The next step forward is finishing the setup for the parabolic mirror trap. The increased light collection efficiency will allow for greater time resolution, which is necessary for further investigation into the time scale of these quantum jumps.

The issue of measurement is not only of interest for its role in the foundations of quantum mechanics, but one which plays an important role in the field of quantum information and quantum computing. The gates in trapped ion quantum computers involve precisely timed laser pulses [14, 15], and the frequency at which these lasers can address the ions depends on how the electrons interact with radiation on a small time scale.

6 Acknowledgements

Thank you to Boris Blinov for his mentorship. Thank you to Jennifer Lilieholm, Tomasz Sakrejda and Liudmila Zhukas for their help in the lab every day, and for giving me the chance to work in their lab. As well, I am enormously grateful to Linda Vilett, Cheryl McDaniel, Subhadeep Gupta, and Gray Rybka for running the REU program, and giving me with this incredible opportunity. Finally, thank you to the NSF for their generous support.

References

[1] *Introduction to Quantum Mechanics.* Prentice Hall, 2005.

[2] A. Einstein, B. Podolsky, and N. Rosen, "Can quantum-mechanical description of physical reality be considered complete?," *Physical Review*, vol. 47, pp. 777–780, may 1935.

[3] J. S. Bell, "On the einstein podolsky rosen paradox," *Physics Publishing Co.*, 1964.

[4] J. von Neumann, *Mathematical Foundations of Quantum Mechanics.* Princeton University Press, 1955.

[5] I. Hugh Everett, *The Many Worlds Interpretation of Quantum Mechanics.* PhD thesis, Princeton University, 1956.

[6] W. H. Zurek, "Decoherence and the transition from quantum to classical," *Physics Today*, 1991.

[7] W. H. Zurek, "Decoherence and the transition from quantum to classical – revisited," 2003.

[8] W. H. Zurek, "Quantum darwinism," 2009.

[9] A. Bassi and G. Ghirardi, "A general argument against the universal validity of the superposition principle," 2000.

[10] S. L. Adler, "Why decoherence has not solved the measurement problem: A response to p. w. anderson," 2001.

[11] C.-K. Chou, *Ion Photon Entanglement in a Parabolic Mirror Trap*. PhD thesis, University of Washington, 2017.

[12] H. Dehmelt, "Quantum jump," *Nature*, vol. 325, pp. 581–581, feb 1987.

[13] C. Auchter, *Toward a Loophole-Free Bell Inequality Violation with Barium Ions*. PhD thesis, University of Washington, 2016.

[14] P. Z. J. I. Cirac, "Quantum computations with cold trapped ions," *Physical Review*, 15 May 1995.

[15] A. Sorensen and K. Molmer, "Entanglement and quantum computation with ions in thermal motion," 2000.